The Curious Case of 2D Isotropic Incompressible Neo-Hookean Composites

Victor Lefèvre[1] · Gilles A. Francfort[2,3] · Oscar Lopez-Pamies[4,5]

Abstract

The homogenized behavior of a hyperelastic composite material is characterized by an effective stored-energy function that is functionally very different from the stored-energy functions that describe the underlying hyperelastic constituents. Over the past two decades, several analytical and computational results suggest that the case of isotropic incompressible Neo-Hookean composites in 2D may be the exception. This Note conjectures that the homogenized behavior of an isotropic hyperelastic solid made of incompressible Neo-Hookean materials is itself an incompressible Neo-Hookean material. To support this conjecture, earlier results are summarized, a new Reuss lower bound is derived, and a set of computational results is presented for the physically relevant cases of a Neo-Hookean matrix filled with random isotropic distributions of rigid and liquid circular particles of identical size.

Keywords Gaussian rubber · Finite deformations · Polyconvexity · Linear PDEs with nonlinear constraints

Mathematics Subject Classification 74B20 · 74Q05 · 74Q20 · 74S05 · 76T20

1 Introduction

While the study of the effective or homogenized linear behavior of composites materials has a long and rich history, that of their nonlinear behavior is much more sparse. In the case of hyperelastic composites, the non-convexity of the stored-energy function is a major hurdle.

✉ O. Lopez-Pamies
pamies@illinois.edu

V. Lefèvre
victor.lefevre@northwestern.edu

G.A. Francfort
gilles.francfort@cims.nyu.edu

[1] Department of Mechanical Engineering, Northwestern University, Evanston, IL 60208, USA

[2] Courant Institute of Mathematical Sciences, 251 Mercer Street, New York, NY 10012, USA

[3] LAGA, Université Paris-Nord, Avenue J.-B. Clément 93430, Villetaneuse, France

[4] Department of Civil and Environmental Engineering, University of Illinois, Urbana–Champaign, IL 61801-2352, USA

[5] Département de Mécanique, École Polytechnique, 91128 Palaiseau, France

Define

$$\overline{W}(\mathbf{F}) = \inf_{\mathbf{k} \in \mathbb{N}^N} \left\{ \inf_{\mathbf{y} \in \mathbf{k}Y_{0\#}} \fint_{\mathbf{k}Y_0} W(\mathbf{X}, \nabla \mathbf{y}) \, d\mathbf{X} \right\}, \tag{1}$$

where $Y_0 = (0,1)^N$, $\mathbf{k}Y_{0\#} = \{\mathbf{y} : \mathbf{y} = \overline{\mathbf{F}}\mathbf{X} + \mathbf{u}, \ \mathbf{u} \in W_0^{1,p}(\mathbf{k}Y_0; \mathbb{R}^N)\}$ stands for the set of admissible deformation fields $\mathbf{y}(\mathbf{X})$ with average gradient $\fint_{\mathbf{k}Y_0} \nabla \mathbf{y} \, d\mathbf{X} = \overline{\mathbf{F}}$ and $\mathbf{k}Y_0$-periodic fluctuations $\mathbf{u}$. That formula has been shown by Braides [1] and Müller [2] (see also [3]) to represent the effective stored-energy function of hyperelastic composite materials with Y_0-periodic microstructure, provided that the local stored-energy function $W(\mathbf{X}, \mathbf{F})$ satisfies, for arbitrary $\mathbf{F}$,

$$\alpha |\mathbf{F}|^p \leq W(\mathbf{X}, \mathbf{F}) \leq \beta(1 + |\mathbf{F}|^p) \tag{2}$$

for some $\alpha > 0$, β, $1 < p < \infty$.

Conditions (2) rule out all incompressible stored-energy functions and many of the popular compressible ones, including any compressible Neo-Hookean material. It is however expected that the formula (1) should apply to all physically sound stored-energy functions. Fully embracing this expectation, we take (1) as the definition for the effective stored-energy function of periodic hyperelastic composites. For the limiting case of incompressible behavior, which is the focus of this work, we include the pointwise incompressibility of the material as a constraint in the admissible set of deformation fields and write

$$\overline{W}(\overline{\mathbf{F}}) = \begin{cases} \inf_{\mathbf{k} \in \mathbb{N}^N} \left\{ \inf_{\mathbf{y} \in \mathbf{k}Y_{0\#}^{inc}} \fint_{\mathbf{k}Y_0} W(\mathbf{X}, \nabla \mathbf{y}) \, d\mathbf{X} \right\} & \text{if } \det \overline{\mathbf{F}} = 1 \\ +\infty & \text{else} \end{cases}, \tag{3}$$

where

$$\mathbf{k}Y_{0\#}^{inc} = \{\mathbf{y} : \det \nabla \mathbf{y} = 1 \text{ a.e.}, \ \mathbf{y} = \overline{\mathbf{F}}\mathbf{X} + \mathbf{u}, \ \mathbf{u} \in W_0^{1,p}(\mathbf{k}Y_0; \mathbb{R}^N)\}.$$

Now, for a given local stored energy function $W(\mathbf{X}, \mathbf{F})$, the resulting effective stored-energy function $\overline{W}(\overline{\mathbf{F}})$ is, in general, functionally very different[1] from $W(\mathbf{X}, \mathbf{F})$. We conjecture that a rare exception to this rule is the case of isotropic incompressible Neo-Hookean composites in 2D. Precisely, we conjecture that for the case of isotropic composites with local stored-energy function

$$W(\mathbf{X}, \mathbf{F}) = \begin{cases} \dfrac{\mu(\mathbf{X})}{2} [\mathbf{F} \cdot \mathbf{F} - 2] & \text{if } \det \mathbf{F} = 1 \\ +\infty & \text{else} \end{cases} \tag{4}$$

in $N = 2$ space dimensions, the effective stored-energy function (3) is Neo-Hookean and that it is given by

$$\overline{W}(\overline{\mathbf{F}}) = \begin{cases} \dfrac{\overline{\mu}}{2} [\overline{\mathbf{F}} \cdot \overline{\mathbf{F}} - 2] & \text{if } \det \overline{\mathbf{F}} = 1 \\ +\infty & \text{else} \end{cases}, \tag{5}$$

---

[1]This is so even in the most specialized case of isotropic incompressible composite materials made of isotropic incompressible constituents, when the resulting effective stored-energy function $\overline{W}(\overline{\mathbf{F}})$, much like the local stored-energy function $W(\mathbf{X}, \mathbf{F})$, admits representations in terms of just $N - 1$ invariants.

where the effective material parameter $\overline{\mu}$ is the effective shear modulus of the corresponding isotropic incompressible linear elastic composite material. In other words,

$$\overline{\mu} = \fint_{Y_0} \mu(\mathbf{X}) \left(1 + e_{12}(\boldsymbol{\chi})(\mathbf{X})\right) \, d\mathbf{X}, \tag{6}$$

where $\boldsymbol{\chi}(\mathbf{X})$ is the Y_0-periodic function that minimizes

$$\int_{Y_0} \mu(\mathbf{X}) e_{kh}(X_2 \mathbf{e}_1 + X_1 \mathbf{e}_2 + \boldsymbol{\psi}) \cdot e_{kh}(X_2 \mathbf{e}_1 + X_1 \mathbf{e}_2 + \boldsymbol{\psi}) \, d\mathbf{X}$$

on $\left\{ \boldsymbol{\psi} \in W^{1,2}(Y_0; \mathbb{R}^2) : \boldsymbol{\psi} \; Y_0\text{-periodic and Div } \boldsymbol{\psi} = 0 \right\}$.

Summary of Earlier Results In the sequel, we provide evidence in support of the above conjecture. In doing so we follow in the footstep of prior studies. In [4] a formula for the effective stored-energy function of a two-phase particulate hyperelastic composite that includes isotropic Neo-Hookean composites in 2D as a special case is derived, yielding an effective stored-energy function of the form (5) with

$$\overline{\mu} = \overline{\mu}^{HS} = \frac{(1-c)\mu_{\mathrm{m}} + (1+c)\mu_{\mathrm{p}}}{(1+c)\mu_{\mathrm{m}} + (1-c)\mu_{\mathrm{p}}} \mu_{\mathrm{m}}, \tag{7}$$

where μ_{m} and μ_{p} stand for the respective shear moduli of the matrix and of the particles and c is the concentration (area fraction) of particles. Remark that the effective material parameter $\overline{\mu}^{HS}$ in (7) agrees with one of the Hashin-Shtrikman (HS) bounds — the lower bound if $\mu_{\mathrm{p}} > \mu_{\mathrm{m}}$, the upper bound otherwise — for the effective shear modulus of two-phase linear elastic composites made of isotropic incompressible constituents. The same result (7) was derived earlier in [5] via a more direct approach.

In [6] a formula for the effective stored-energy function of a Neo-Hookean matrix filled with a random isotropic distribution of rigid particles in 2D is obtained. The result is again of the Neo-Hookean form (5). There,

$$\overline{\mu} = \overline{\mu}^{DS} = \frac{\mu_{\mathrm{m}}}{(1-c)^2}, \tag{8}$$

where, as above, μ_{m} stands for the shear modulus of the underlying Neo-Hookean matrix. Interestingly, $\overline{\mu}^{DS}$ in (8) agrees with the classical result generated by the so-called differential scheme for the effective shear modulus of a linear elastic isotropic incompressible material filled with a random distribution of circular rigid particles of infinitely many sizes.

In a more computational direction, finite-element (FE) solutions for the effective stored-energy function of two-phase Neo-Hookean composites made of the periodic repetition of a square unit cell $Y_0 = (0, 1)^2$ containing 60 randomly distributed circular almost-rigid particles of identical (monodisperse) size were generated in [7] under the assumption that the minimizers in (1) are Y_0-periodic. While such microstructures are not exactly isotropic, the relatively large number of particles (more on this below) led to fairly isotropic responses, at least for the composites with small-to-moderate particle concentration ($c \leq 0.3$). The comprehensive bifurcation studies in [8] later established that the assumption that the minimizers for the type of Neo-Hookean composites studied in [7] are Y_0-periodic is indeed justified. Furthermore [6] showed that the FE solutions put forth in [7] were, by and large, of Neo-Hookean form.

More recently, FE solutions for the effective stored-energy function (3) of a variety of two-phase particulate Neo-Hookean composites with either rigid ($\mu_p = +\infty$) or liquid ($\mu_p = 0+$) particles have been obtained in [9]. The resulting effective stored-energy functions appear to be Neo-Hookean as well.

The organization of the rest of this Note is as follows. In Sect. 2, we recall the classical Voigt upper and Reuss lower bounds and derive a new Reuss bound for the effective stored-energy function (3) when specialized to isotropic incompressible Neo-Hookean composites with local stored-energy function (4). Both the Voigt and new Reuss bounds are shown to be consistent with the conjecture (5). In Sect. 3, we present a comprehensive set of numerical solutions for (3) for the physically relevant cases of a Neo-Hookean matrix filled with random isotropic distributions of rigid — infinite shear stiffness — and liquid — incompressible with vanishingly small shear stiffness — circular particles of monodisperse size. The results span a large range of concentrations of particles, $c \in [0, 0.60]$. All of them seem to reinforce the conjecture (5).

From now onward, we tacitly assume that $\det \overline{\mathbf{F}} = 1$ and that $N = 2$.

2 Voigt and Reuss Bounds

The Classical Voigt Bound The Voigt upper bound is trivial. It suffices to consider as admissible trial field in (3) the field $\mathbf{y}(\mathbf{X}) = \overline{\mathbf{F}}\mathbf{X}$. This yields

$$\overline{W}(\overline{\mathbf{F}}) \leq \frac{\overline{\mu}^V}{2}\left[\overline{\mathbf{F}} \cdot \overline{\mathbf{F}} - 2\right] \qquad \text{with} \qquad \overline{\mu}^V := \fint_{Y_0} \mu(\mathbf{X})\, d\mathbf{X}. \tag{9}$$

The Classical Reuss Bound Establishing Reuss lower bounds usually requires a dual formulation of the minimization problem (3). But the lack of convexity stands in the way of that approach. This difficulty can be circumvented by using appropriate types of Legendre transforms [10]. Using the standard Legendre transform

$$W^\star(\mathbf{X}, \mathbf{S}) := \sup_{\mathbf{F}} \{\mathbf{S} \cdot \mathbf{F} - W(\mathbf{X}, \mathbf{F})\} = \frac{1}{2\mu(\mathbf{X})}\mathbf{S} \cdot \mathbf{S} + \mu(\mathbf{X}),$$

we get

$$\frac{\mu(\mathbf{X})}{2}[\mathbf{F} \cdot \mathbf{F} - 2] \geq \mathbf{S} \cdot \mathbf{F} - \frac{1}{2\mu(\mathbf{X})}\mathbf{S} \cdot \mathbf{S} - \mu(\mathbf{X})$$

for arbitrary $\mathbf{S}$. Substitution in the homogenization formula (3) leads to

$$\overline{W}(\overline{\mathbf{F}}) \geq \inf_{\mathbf{k} \in \mathbb{N}^2} \left\{ \inf_{\mathbf{y} \in \mathbf{k}Y_{0\#}} \fint_{\mathbf{k}Y_0} \left(\mathbf{S} \cdot \mathbf{F} - \frac{1}{2\mu(\mathbf{X})}\mathbf{S} \cdot \mathbf{S} - \mu(\mathbf{X}) \right) d\mathbf{X} \right\}.$$

Since this inequality is valid for arbitrary $\mathbf{S}$, we can choose it to be a constant, say $\mathbf{S} = \overline{\mathbf{S}}$. For this choice, the inequality simplifies to

$$\overline{W}(\overline{\mathbf{F}}) \geq \overline{\mathbf{S}} \cdot \overline{\mathbf{F}} - \frac{1}{2}\left(\fint_{Y_0} \frac{1}{\mu(\mathbf{X})}\, d\mathbf{X} \right) \overline{\mathbf{S}} \cdot \overline{\mathbf{S}} - \fint_{Y_0} \mu(\mathbf{X})\, d\mathbf{X},$$

where we have made use of the fact that $\fint_{\mathbf{k}Y_0} \nabla \mathbf{y}(\mathbf{X}) \, d\mathbf{X} = \overline{\mathbf{F}}$ and of the Y_0-periodicity of $\mu(\mathbf{X})$. Optimizing this result with respect to $\overline{\mathbf{S}}$ finally leads to the classical Reuss bound

$$\overline{W}(\overline{\mathbf{F}}) \geq \frac{\overline{\mu}^R}{2} \overline{\mathbf{F}} \cdot \overline{\mathbf{F}} - \overline{\mu}^V \qquad \text{with} \qquad \overline{\mu}^R := \left(\fint_{Y_0} \frac{1}{\mu(\mathbf{X})} \, d\mathbf{X} \right)^{-1} \tag{10}$$

for Neo-Hookean composites, where $\overline{\mu}^V$ is given by $(9)_2$.

Given that $\overline{\mu}^V \geq \overline{\mu}^R$, the Reuss bound (10) violates the trivial bound $\overline{W}(\overline{\mathbf{F}}) \geq 0$ for small deformations ($\overline{\mathbf{F}} \to \mathbf{I}$). Further, the Reuss bound (10) is unbounded from below for the limiting case when one of the phases is rigid, for $\overline{\mu}^V = +\infty$ then. In the opposite extreme case when one of the phases is a liquid, the Reuss bound (10) becomes $-\overline{\mu}^V$ since $\overline{\mu}^R = 0$.

The New Reuss Bound To improve on (10), we consider a different transformation inspired by, e.g., [11]. Precisely, we introduce

$$\Psi^\star(\mathbf{X}, \mathbf{S}, p) = \sup_{\mathbf{F}} \left\{ \mathbf{S} \cdot \mathbf{F} + p \det \mathbf{F} - \frac{\mu(\mathbf{X})}{2} \mathbf{F} \cdot \mathbf{F} \right\} \tag{11}$$

and remark that, upon writing $\mathbf{F}$ as a 4-vector, i.e., $\mathbf{F} = \begin{pmatrix} F_{11} \\ F_{22} \\ F_{12} \\ F_{21} \end{pmatrix}$, $\Psi^\star(\mathbf{X}, \mathbf{S}, p)$ reads as

$$\Psi^\star(\mathbf{X}, \mathbf{S}, p) = \sup_{\mathbf{F}} \{ \mathbf{S} \cdot \mathbf{F} + \mathbf{F} \cdot \mathcal{M} \mathbf{F} \} \qquad \text{with}$$

$$\mathcal{M} := \begin{pmatrix} -\mu(\mathbf{X})/2 & p/2 & 0 & 0 \\ p/2 & -\mu(\mathbf{X})/2 & 0 & 0 \\ 0 & 0 & -\mu(\mathbf{X})/2 & -p/2 \\ 0 & 0 & -p/2 & -\mu(\mathbf{X})/2 \end{pmatrix}.$$

Note that the eigenvalues m_i, $i = 1, \ldots, 4$ of $\mathcal{M}$ are all non positive iff $p^2 \leq \mu^2(\mathbf{X})$.

Now, take $p = \mu(\mathbf{X})$, then $\mathbf{F} \cdot \mathcal{M} \mathbf{F} = -\frac{\mu(\mathbf{X})}{2} \left[(F_{11} - F_{22})^2 + (F_{12} + F_{21})^2 \right]$, so

$$\Psi^\star(\mathbf{X}, \mathbf{S}, \mu(\mathbf{X})) = \sup_{\mathbf{F}} \left\{ \mathbf{S} \cdot \mathbf{F} - \frac{\mu(\mathbf{X})}{2} \left[(F_{11} - F_{22})^2 + (F_{12} + F_{21})^2 \right] \right\}$$

$$= \begin{cases} +\infty & \text{if } S_{11} + S_{22} \neq 0 \text{ or } S_{12} - S_{21} \neq 0 \\ \dfrac{1}{8\mu(\mathbf{X})} \left[(S_{11} - S_{22})^2 + (S_{12} + S_{21})^2 \right] & \text{else} \end{cases}$$

Consequently, since, from (11), $\dfrac{\mu(\mathbf{X})}{2} [\mathbf{F} \cdot \mathbf{F} - 2] \geq \mathbf{S} \cdot \mathbf{F} + \mu(\mathbf{X}) \det \mathbf{F} - \Psi^\star(\mathbf{X}, \mathbf{S}, \mu(\mathbf{X})) - \mu(\mathbf{X})$, substituting in the homogenization formula (3), choosing $\mathbf{S} = \begin{pmatrix} \alpha & \beta \\ \beta & -\alpha \end{pmatrix}$ with arbitrary constants α and β, and exploiting the facts that $\det \overline{\mathbf{F}} = 1$, $\fint_{\mathbf{k}Y_0} \nabla \mathbf{y}(\mathbf{X}) \, d\mathbf{X} = \overline{\mathbf{F}}$, and that $\mu(\mathbf{X})$ is Y_0-periodic leads to

$$\overline{W}(\overline{\mathbf{F}}) \geq \sup_{\alpha, \beta} \left\{ \fint_{Y_0} \left(\alpha(\overline{F}_{11} - \overline{F}_{22}) + \beta(\overline{F}_{12} + \overline{F}_{21}) - \frac{1}{2\mu(\mathbf{X})} (\alpha^2 + \beta^2) \right) d\mathbf{X} \right\}$$

$$= \frac{\overline{\mu}^R}{2} \left[\overline{\mathbf{F}} \cdot \overline{\mathbf{F}} - 2 \right], \tag{12}$$

which is precisely the new Reuss bound.

Note that, like its upper counterpart (9), the new Reuss bound (12) is of Neo-Hookean form and its effective material parameter $\overline{\mu}^R$ agrees identically with the classical Reuss bound for the effective shear modulus of linear elastic composites made of isotropic incompressible constituents.

Remark 1 A corollary that immediately follows from the Voigt upper bound (9) and the Reuss lower bound (12) is that the effective stored-energy function for Neo-Hookean composites with local shear modulus $\mu(\mathbf{X}) = \mu_0 + t\, w(\mathbf{X})$, $|w(\mathbf{X})| < C$, is identically Neo-Hookean and asymptotically given by

$$\overline{W}(\overline{\mathbf{F}}) = \frac{1}{2} \left(\mu_0 + t \fint_{Y_0} w(\mathbf{X})\, d\mathbf{X} \right) \left[\overline{\mathbf{F}} \cdot \overline{\mathbf{F}} - 2 \right] + O(t^2) \tag{13}$$

in the limit of small heterogeneity contrast as $t \to 0$. This is so because $\overline{\mu}^R = \overline{\mu}^V + O(t^2)$.

3 Computational Results for a Neo-Hookean Matrix Filled with Circular Rigid and Liquid Particles

In this section, which complements the small-contrast result (13), we present computational results for the effective stored-energy function (3) for two physically relevant classes of isotropic Neo-Hookean composites with infinite heterogeneity contrast, those of a Neo-Hookean matrix filled with either rigid or liquid circular particles of monodisperse size.

3.1 Construction of the Microstructures

We begin by outlining the process by which we constructed and pre-selected the microstructures and then describe the numerical method of solution and the final filtering procedure used to identify the microstructures that lead to elastic behaviors that are indeed isotropic to a sufficiently high degree of accuracy.

In the spirit of [12–14], the type of isotropic particulate composite materials considered in this section is approximated as an infinite medium made of the periodic repetition of a unit cell containing a random distribution of a sufficiently large but *finite* number N of particles. A critical issue in such an approach is the determination of that sufficiently large number N. Equally critical is the choice of an appropriate numerical scheme that will handle large deformations, the incompressibility constraint, and the large deformation gradients that arise between closely packed particles.

So as to be able to cover a large range of particle concentrations, we made use of the algorithm introduced by Lubachevsky and Stillinger [15]. Although this algorithm allows to generate microstructures spanning the full range of concentrations — from the dilute limit $c \searrow 0$ to the percolation threshold $c \nearrow c_p \approx 0.90$ [15] — we did not wish to deal with the computational challenges of extremely packed microstructures here and restricted our attention to the range $c \in [0, 0.60]$. Moreover, we imposed the minimal distance between any pair of particles to be greater than 1% of their radius.

We begun by generating a total of 4000 realizations of square unit cells $Y_0 = (-1/2, 1/2)^2$ containing 30, 60, 120, 240, 480, 960 randomly distributed particles. For
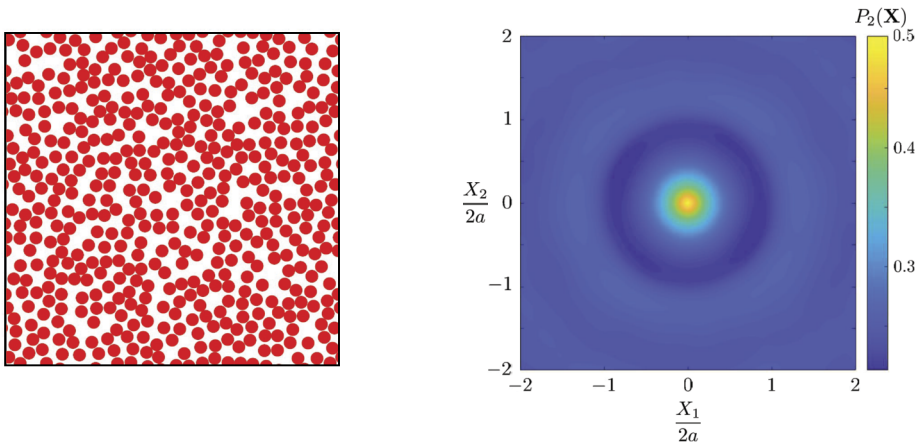
Fig. 1 Representative unit cell Y_0 containing a random distribution of $\mathtt{N} = 480$ monodisperse circular particles at concentration $c = 0.50$ and the contour plot of its two-point correlation function $P_2(\mathbf{X})$ near the origin $\mathbf{X} = \mathbf{0}$ as a function of the coordinates X_1 and X_2 normalized by the diameter $2a$ of the particles

each realization, we computed the two-point correlation function $P_2(\mathbf{X}) = \oint_{Y_0} \theta(\mathbf{X}')\theta(\mathbf{X} + \mathbf{X}')\, d\mathbf{X}'$, where $\theta(\mathbf{X}')$ stands for the characteristic function of the particles, that is, $\theta(\mathbf{X}) = 1$ if $\mathbf{X}$ lies within a particle and zero otherwise. As a first assessment of deviation from exact geometric isotropy (which is only achieved in the limit of infinitely many particles), we then computed the deviation of $P_2(\mathbf{X})$ from its isotropic projection $I_2(|\mathbf{X}|) = 1/(2\pi) \int_0^{2\pi} P_2(|\mathbf{X}|\cos\phi\,\mathbf{e}_1 + |\mathbf{X}|\sin\phi\,\mathbf{e}_2)\, d\phi$ onto the space of functions that depend on $\mathbf{X}$ only through its magnitude $|\mathbf{X}|$ ($\{\mathbf{e}_1, \mathbf{e}_2\}$ stand for the principal axes of the square unit cell Y_0). Realizations that did not satisfy the condition

$$\frac{||P_2(\mathbf{X}) - I_2(|\mathbf{X}|)||_1}{||I_2(|\mathbf{X}|)||_1} \leq 2 \times 10^{-2} \tag{14}$$

were discarded as not sufficiently isotropic. This filtering process reduced the initial set of 4000 realizations to just a set of 80 potentially acceptable realizations, 10 for each of the 8 concentrations

$$c = 0.01, 0.05, 0.10, 0.20, 0.30, 0.40, 0.50, 0.60$$

that we chose as a discretization of the range $c \in [0, 0.60]$. By way of an example, Fig. 1 shows a representative unit cell Y_0 containing a total of $\mathtt{N} = 480$ particles at concentration $c = 0.50$ that satisfied the condition (14) alongside a contour plot of its two-point correlation function.

Remark 2 The criterion (14) provides a computationally inexpensive tool to weed out microstructures that cannot lead to isotropic elastic behaviors. However, microstructures that do satisfy (14) need not exhibit isotropic elastic behaviors. As described further below, a thorough direct check of its constitutive behavior is required to establish whether a Neo-Hookean composite with a *finite* number $\mathtt{N}$ of particles does indeed exhibit isotropic elastic behavior to within the desired tolerance.

We then computed the effective stored-energy function of the particulate Neo-Hookean composites with the above-outlined 80 potentially acceptable microstructures. Specifically, we used the *discretized* parametrization[2]

$$\overline{\mathbf{F}}_{\varphi}(\lambda) = \lambda \cos\varphi\,\mathbf{e}_1 \otimes \mathbf{e}_1 - \lambda \sin\varphi\,\mathbf{e}_1 \otimes \mathbf{e}_2 + \lambda^{-1}\sin\varphi\,\mathbf{e}_2 \otimes \mathbf{e}_1 + \lambda^{-1}\cos\varphi\,\mathbf{e}_2 \otimes \mathbf{e}_2 \quad (15)$$

in terms of the two parameters $\lambda \in \mathbb{R}$ and $\varphi \in \{0, \pi/8, \pi/4, 3\pi/8, \pi/2\}$ for the applied average deformation gradient $\overline{\mathbf{F}}$. Physically, this corresponds to pure shear deformations with stretches λ and λ^{-1} at an angle φ with respect to the principal axes $\{\mathbf{e}_1, \mathbf{e}_2\}$ of the unit cell Y_0. For the spatial discretization, we employed the open-source mesh generator code Gmsh [16] to discretize the unit cells with non-overlapping 6-node triangular elements. Because of the incompressibility of the matrix material and that of the rigid and liquid particles, we made use of a hybrid re-formulation of the variational problem (3) in which both the displacement field $\mathbf{y}$ and a pressure field p are the independent fields in the problem (see, e.g., Sect. 5 in [17]). Furthermore, the constitutive behavior of the rigid particles was described as a set of kinematic constraints over their boundaries and so their interior did not require meshing [18]. The constitutive behavior of the liquid particles was described by a Neo-Hookean stored-energy function with a shear modulus that was two orders of magnitude softer than that of the matrix, namely, $\mu_{\mathrm{p}} = \mu_{\mathrm{m}}/100$. Within the hybrid re-formulation, we made use of triangular elements featuring approximations that are quadratic in the deformation field and linear in the pressure field. In agreement with the bifurcation analysis in [8], all generated FE solutions were Y_0-periodic.

With the FE solutions at hand, the final step was to identify which of the pre-selected 80 microstructures did indeed exhibit elastic responses that were isotropic to a sufficiently high degree of accuracy. To that end, we checked whether the inequality

$$\frac{\max\limits_{\varphi}\left\{\overline{W}(\overline{\mathbf{F}}_{\varphi}(\lambda))\right\} - \min\limits_{\varphi}\left\{\overline{W}(\overline{\mathbf{F}}_{\varphi}(\lambda))\right\}}{\min\limits_{\varphi}\left\{\overline{W}(\overline{\mathbf{F}}_{\varphi}(\lambda))\right\}} \leq 10^{-2} \quad (16)$$

was satisfied. Out of the 10 pre-selected microstructures for each of the 8 concentrations $c = 0.01, 0.05, 0.10, 0.20, 0.30, 0.40, 0.50, 0.60$, only a few satisfied (16) for each c. As we show next, the effective stored-energy functions for the Neo-Hookean composites with those microstructures appear to be of Neo-Hookean form.

3.2 Results

Figure 2(a) presents plots of the FE results (solid circles/dashed lines) for the effective stored-energy functions (3) of the Neo-Hookean composites with concentrations $c = 0.10, 0.30$, and 0.50 of circular rigid particles. The results are normalized by the initial shear modulus μ_{m} of the underlying Neo-Hookean matrix as a function of the deformation measure $\overline{I}_1 = \overline{\mathbf{F}} \cdot \overline{\mathbf{F}} = \lambda^2 + \lambda^{-2}$.

For direct comparison, Fig. 2(a) includes the results (solid lines) given by the conjecture (5). Figure 2(b) presents plots of the effective shear modulus $\overline{\mu}$ in that formula, as defined

---

[2]Thanks to its objectivity $\overline{W}(\mathbf{Q}\overline{\mathbf{F}}) = \overline{W}(\overline{\mathbf{F}})\ \forall \mathbf{Q} \in Orth^+$ and incompressibility $\overline{W}(\overline{\mathbf{F}}) = +\infty$ if $\det\overline{\mathbf{F}} \neq 1$, the effective stored-energy function (3) admits representations in terms of two scalar variables, this regardless of its anisotropy. In this work, we found it convenient to use the representation $\overline{\Psi}(\lambda, \varphi) := \overline{W}(\overline{\mathbf{F}}_{\varphi}(\lambda))$, where $\overline{\mathbf{F}}$ is given by (15) with $\lambda \in \mathbb{R}$ and $\varphi \in [0, \pi/2]$. In our calculations, we discretized the latter range as $\varphi \in \{0, \pi/8, \pi/4, 3\pi/8, \pi/2\}$.
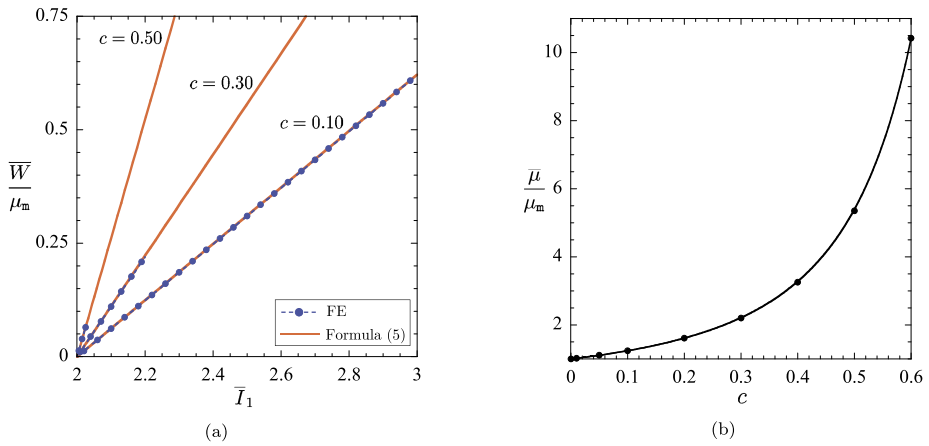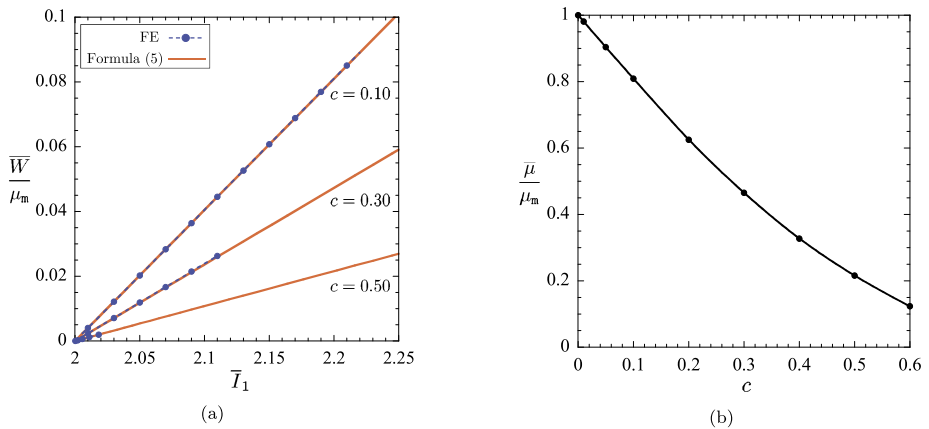
Fig. 2 (**a**) FE results for the effective stored-energy function (3) for Neo-Hookean composites made of a Neo-Hookean matrix filled with circular rigid ($\mu_\mathrm{p} = +\infty$) particles at several concentrations c as functions of the deformation measure $\overline{I}_1 = \overline{\mathbf{F}} \cdot \overline{\mathbf{F}}$. (**b**) The corresponding effective shear modulus (6) in the conjectured formula (5), which is also plotted in part (**a**) for direct comparison with the FE results, as a function of c

Fig. 3 (**a**) FE results for the effective stored-energy function (3) for Neo-Hookean composites made of a Neo-Hookean matrix filled with circular liquid ($\mu_\mathrm{p} = \mu_\mathrm{m}/100$) particles at several concentrations c as functions of the deformation measure $\overline{I}_1 = \overline{\mathbf{F}} \cdot \overline{\mathbf{F}}$. (**b**) The corresponding effective shear modulus (6) in the conjectured formula (5), which is also plotted in part (**a**) for direct comparison with the FE results, as a function of c

by (6) and computed by FE. In particular, the results for $\overline{\mu}$ are shown normalized by the initial shear modulus μ_m of the underlying Neo-Hookean matrix as a function of the concentration of particles c for the values $c = 0.01, 0.05, 0.10, 0.20, 0.30, 0.40, 0.50, 0.60$ that we examined.

It is evident from Fig. 2 that the effective stored-energy functions for Neo-Hookean composites made of a Neo-Hookean matrix filled with circular rigid particles seem to be precisely of Neo-Hookean form and, in particular, given by (5).

While the maximum applied deformations, measured by $\overline{I}_1$, are not exceedingly large in the results presented in Fig. 2(a), we emphasize that the local stretches in the underlying

Neo-Hookean matrix are large. Because the particles are rigid and thus do not deform, the matrix must deform more than the applied average deformation. In other words, the FE results in Fig. 2(a) fully probe the nonlinear elasticity of the underlying Neo-Hookean matrix despite the deceivingly moderate values of $\overline{I}_1$.

Figure 3 shows results for liquid particles that are entirely analogous to those in Fig. 2. The main observation remains the same as that for Fig. 2.

References

1. Braides, A.: Homogenization of some almost periodic coercive functional. Accad. Naz. Sci. XL **103**, 313–322 (1985)
2. Müller, S.: Homogenization of nonconvex integral functionals and cellular elastic materials. Arch. Ration. Mech. Anal. **99**, 189–212 (1987)
3. Braides, A., Defranceschi, A.: Homogenization of Multiple Integrals. Springer, Berlin (1999)
4. Lopez-Pamies, O., Idiart, M.I.: Fiber-reinforced hyperelastic solids: a realizable homogenization constitutive theory. J. Eng. Math. **68**, 57–83 (2010)
5. deBotton, G.: Transversely isotropic sequentially laminated composites in finite elasticity. J. Mech. Phys. Solids **53**, 1334–1361 (2005)
6. Lopez-Pamies, O.: An exact result for the macroscopic response of particle-reinforced Neo-Hookean solids. J. Appl. Mech. **77**, 021016 (2010)
7. Moraleda, J., Segurado, J., Llorca, J.: Finite deformation of incompressible fiber-reinforced elastomers: a computational micromechanics approach. J. Mech. Phys. Solids **57**, 1596–1613 (2009)
8. Michel, J.C., Lopez-Pamies, O., Ponte Castañeda, P., Triantafyllidis, N.: Microscopic and macroscopic instabilities in finitely strained fiber-reinforced elastomers. J. Mech. Phys. Solids **58**, 1776–1803 (2010)
9. Lefèvre, V., Danas, K., Lopez-Pamies, O.: A general result for the magnetoelastic response of isotropic suspensions of iron and ferrofluid particles in rubber, with applications to spherical and cylindrical specimens. J. Mech. Phys. Solids **107**, 343–364 (2017)
10. Willis, J.R.: The overall elastic response of composite materials. J. Appl. Mech. **50**, 1202–1209 (1983)
11. Kohn, R.V., Strang, G.: Optimal design and relaxation of variational problems, II. Commun. Pure Appl. Math. **39**, 139–182 (1986)
12. Gusev, A.A.: Representative volume element size for elastic composites: a numerical study. J. Mech. Phys. Solids **45**, 1449–1459 (1997)
13. Michel, J.C., Moulinec, H., Suquet, P.: Effective properties of composite materials with periodic microstructure: a computational approach. Comput. Methods Appl. Mech. Eng. **172**, 109–143 (1999)
14. Lopez-Pamies, O., Goudarzi, T., Danas, K.: The nonlinear elastic response of suspensions of rigid inclusions in rubber: II — a simple explicit approximation for finite-concentration suspensions. J. Mech. Phys. Solids **61**, 19–37 (2013)
15. Lubachevsky, B.D., Stillinger, F.H.: Geometric properties of random disk packings. J. Stat. Phys. **60**, 561–583 (1990)
16. Geuzaine, C., Remacle, J-F.: Gmsh: a 3-D finite element mesh generator with built-in pre- and post-processing facilities. Int. J. Numer. Methods Eng. **79**, 1309–1331 (2009)
17. Lefèvre, V., Lopez-Pamies, O.: Nonlinear electroelastic deformations of dielectric elastomer composites: II — non-Gaussian elastic dielectrics. J. Mech. Phys. Solids **99**, 438–470 (2017)
18. Chi, H., Lopez-Pamies, O., Paulino, G.H.: A variational formulation with rigid-body constraints for finite elasticity: theory, finite element implementation, and applications. Comput. Mech. **57**, 325–338 (2016)